

lations; this is Ecker and Müller's result. Curve 3 is the result of the present theory, which is seen to lie almost halfway in between the other two. Indeed, were one to use

$$\lambda'' = (\kappa T / 6\pi n e^2)^{\frac{1}{2}} \quad (28)$$

as a shielding length, and no pair correlations, one would obtain a very accurate result. It must be pointed out that the error in Ecker and Müller's distributions is actually small; all three curves in Fig. 3 are much closer together than they are to the Holtmark distribution. Work similar to that of Ecker and Müller has also been done by Hoffman and Theimer,<sup>7</sup> but their numerical accuracy is inferior to that of the former authors.

Work on field distributions at a charged point has also been done by Broyles<sup>8</sup> and Lewis and Margenau.<sup>6</sup> The latter authors used an unshielded field, hence their work should be compared with results on the high-

<sup>7</sup> H. Hoffman and O. Theimer, *Astrophys. J.* **127**, 477 (1958).

<sup>8</sup> A. A. Broyles, *Phys. Rev.* **100**, 1181 (1955); *Z. Physik* **151**, 187 (1958).

frequency component. This is the case where the pair term was found here to be quite important. This pair term is not included by Lewis and Margenau, so that their results differ appreciably from those of the present work, their distribution being shifted toward larger fields. The work of Broyles is hard to compare with others as it does not yield the Holtmark distribution in the limit of small  $r_0/\lambda$ ; this work would be useful for large values of  $r_0/\lambda$ , when the cluster expansion fails completely.

#### ACKNOWLEDGMENTS

The authors are indebted to H. Griem and A. C. Kolb for pointing out a serious mistake in an earlier version of the theory, as well as for many fruitful discussions. They also wish to thank A. Broyles for several communications. Some of the calculations were performed on an IBM 704 which was kindly made available by the International Business Machines Corporation and the Westinghouse Electric Corporation; this essential help is gratefully acknowledged.

## Nuclear Quadrupole Spin-Lattice Relaxation in Alkali Halides\*

E. G. WIKNER,† W. E. BLUMBERG,‡ AND E. L. HAHN

*Department of Physics, University of California, Berkeley, California*

(Received November 25, 1959)

Nuclear quadrupole spin-lattice relaxation times have been measured in alkali halide crystals by the pulsed magnetic resonance technique. Measurements were made on Na<sup>23</sup> in NaCl, NaBr, and NaI; Cl<sup>35</sup> in NaCl and KCl; Br<sup>79,81</sup> in NaBr, KBr, RbBr, and CsBr; Rb<sup>87</sup> in RbCl and RbBr; and I<sup>127</sup> in NaI, KI, and CsI. Over a temperature range of 298°K to 195°K the relaxation times are inversely proportional to the square of the absolute temperature. The data are compared to relaxation times calculated from an ionic crystal model of Van Kranendonk and a covalent model of Yosida and Moriya. The ionic model is modified to include the interaction between the nuclear quadrupole moment and the electric field gradient due to electric dipole moments associated with optical modes of vibration. Neither of these models alone predicts the experimental relaxation times for all cases, but a combination of the two effects is required. The modified ionic model applies reasonably well to crystals which contain the lighter ions.

### I. INTRODUCTION

TWO theories have been proposed to explain nuclear quadrupole spin-lattice relaxation times  $T_1$  in crystalline solids. The relaxation due to fluctuations of the electric field gradient originating from ionic point charges is considered in the theory of Van Kranendonk,<sup>1</sup> referred to as the ionic model. The theory of Yosida and Moriya,<sup>2</sup> which applies a covalent model, attributes relaxation to the asymmetry of the electron charge cloud distribution when two

ions are in a state of covalent bonding. These theories were applied to the alkali halides and our interest will be confined to these crystals. A recent attempt<sup>3</sup> to interpret relaxation-time data in terms of these models was inconclusive because of the lack of sufficient data. With the enlarged data presented in this paper, we attempt to confirm, in various cases, the proper combination of mechanisms that couple the nuclear quadrupole moment to the lattice-phonon distribution in the temperature region above the Debye temperature.

An important modification of the ionic model, calculated by one of the authors (W.E.B.), introduces the effect of induced electric dipole moments associated with optical modes of the lattice vibration. This

\* Supported by the Office of Naval Research and the National Security Agency.

† Present address: General Atomics, San Diego, California.

‡ Present address: Bell Telephone Laboratories, Murray Hill, New Jersey.

<sup>1</sup> J. Van Kranendonk, *Physica* **20**, 781 (1954).

<sup>2</sup> K. Yosida and T. Moriya, *J. Phys. Soc. (Japan)* **11**, 33 (1956).

<sup>3</sup> E. G. Wikner and T. P. Das, *Phys. Rev.* **109**, 360 (1958).

additional degree of freedom is incorporated into the point charge model of Van Kranendonk.

## II. EXPERIMENTAL RESULTS

Magnetic resonance pulse techniques<sup>4</sup> were used in our measurements because they afford a direct determination of nuclear spin-lattice relaxation times  $T_1$ . The inference of relaxation times by the continuous wave (c.w.) saturation method is difficult in solids because of complications involving line-shape interpretation. The c.w. method, however, is useful for the observation of the recovery of nuclear magnetization toward thermal equilibrium by an adiabatic fast passage measurement<sup>5</sup> following initial spin saturation at an earlier time  $\tau$ . This can be done only if  $T_1$  is conveniently long. The pulse method in this investigation measures  $T_1$  values ranging from 0.01 sec to 12 sec. For the short  $T_1$  measurements, less than 1 sec, a 90°-90° two-pulse sequence was employed. At  $t=0$ , the magnitude of a free nuclear induction signal following a short radiofrequency pulse, having typically a width of 40  $\mu$ sec and a rotating field component  $H_1$  of approximately 14 gauss, provides a measure of  $M_0$ , the nuclear magnetization at thermal equilibrium. A second 90° pulse follows at a time  $\tau$  later, when  $\tau$  is much greater than the free-precession decay time  $T_2$ , giving a signal that measures the exponential recovery toward thermal equilibrium. A "picket-90°" pulse method was convenient for  $T_1$  measurements exceeding 1 sec. The initial saturation is produced by a series of approximate 90° pulses occurring in rapid succession, separated from one another by a time which is greater than  $T_2$  and much shorter than  $T_1$ . This picket sequence assures complete initial nuclear saturation without the necessity of obtaining an exact 90° condition for the initial single 90° pulse or on the following 90° pulse. These 90° conditions are difficult to obtain for slow repetition rates.

Experiments were performed with optically pure single crystals obtained from Harshaw Chemical Company, except for NaBr, RbBr, and NaI which were grown from our own melt system, and for RbCl, which was a polycrystalline sample. Depending upon their gyromagnetic ratios, nuclei were studied at Larmor frequencies of 12 Mc/sec and 4.5 Mc/sec provided by a pulsed oscillator. The pulse from this oscillator has a rise-and-fall time of 2  $\mu$ sec, with a peak-to-peak amplitude of 3000 volts. A nonoverloading wide-band amplifier<sup>6</sup> is used as a receiver and is decoupled from the transmitter by use of a cross-coil arrangement that minimizes receiver saturation. The transmitter coil is wound in the form of a Helmholtz coil pair, each of which is slightly elliptical in shape in order to provide a more homogeneous rf field over the sample. The

receiver coil is wrapped directly around the sample. The receiver recovers completely within 10  $\mu$ sec after the trailing edge of the oscillator pulse is clamped. The receiver output is coupled through a high-gain tuned detector, and the final signal enters a dual channel "boxcar" narrow-band integrator,<sup>7</sup> which then connects to a Brown recorder.

The experimental results are presented in Table I. Each relaxation time was measured at least 5 times, and the tabulated results are the average of these measurements. Their accuracy is within 10% unless otherwise stated. The orientation of crystalline axes with respect to the applied field  $H_0$  is not specified because no dependence of  $T_1$  upon orientation was observed for any nucleus.

Certain overall conclusions can be drawn from an inspection of the data. Above all, the nuclear lattice-phonon interactions are definitely quadrupolar in nature for the following reasons.

1. In relaxation processes, the transition probability is directly proportional to the square of the matrix elements<sup>8</sup> connecting two levels of the spin system. In our case the relaxation times prove to be inversely proportional to the square of the quadrupole moments of two isotopes in the same crystal. For example, the thermal relaxation time ratio  $T_1(\text{Br}^{79})/T_1(\text{Br}^{81})$  of the  $\text{Br}^{79}$  and  $\text{Br}^{81}$  isotopes is measured to within 5% of the calculated ratio of the inverse square of their quadrupole moments, 1.4, in the four cases of NaBr, KBr, RbBr, and CsBr.

TABLE I. Experimental  $T_1$  results.

Crystal	Nucleus	$Q$ (barns)	$T_1$ (sec)	Temp(°K)
NaCl	Na <sup>23</sup>	0.10	12	298
			14.5	273
			28	195
NaBr	Na <sup>23</sup>	0.10	6.0	298
			5.0	298
			5.2	298
NaCl	Cl <sup>35</sup>	-0.078	8.5	298
			8.5	298
NaBr	Br <sup>79</sup>	0.33	0.050	298
			0.071	298
KBr	Br <sup>79</sup>	0.33	0.072	298
			0.087	273
			0.166	195
	Br <sup>81</sup>	0.28	0.103	298
			0.122	273
			0.230	195
CsBr	Br <sup>79</sup>	0.33	0.080	298
			0.115	298
RbCl	Rb <sup>87</sup>	0.15	0.250	298
RbBr	Br <sup>87</sup>	0.15	0.165	298
			0.33	0.065±0.040
NaI	I <sup>127</sup>	-0.59	0.100±0.050	298
			0.012	298
KI	I <sup>127</sup>	-0.59	0.019	298
			0.023	273
			0.045	195
			0.010	298
CsI	I <sup>127</sup>	-0.59	0.010	298

<sup>4</sup> E. L. Hahn, Phys. Rev. **80**, 580 (1950).

<sup>5</sup> F. Bloch, Phys. Rev. **70**, 460 (1946).

<sup>6</sup> R. J. Blume (private communication).

<sup>7</sup> D. F. Holcomb and R. E. Norberg, Phys. Rev. **98**, 1074 (1955); D. E. Kaplan, Ph.D. thesis, University of California, 1958 (unpublished).

<sup>8</sup> R. V. Pound, Phys. Rev. **79**, 685 (1950).

2. The suspicion that relaxation may be partly due to paramagnetic ions<sup>9</sup> was eliminated in the following manner. The Na<sup>23</sup> relaxation time was measured in an *F*-center doped NaCl crystal. Although the crystal was noticeably colored, the  $T_1$  value of 12 sec at 298°K was unchanged from that obtained from an optically pure, undoped sample. This characteristic has also been found to be true for other nuclei.<sup>10</sup> Also, if the fractional concentration in the number of ion impurities is less than  $10^{-5}$ , it has been found<sup>11</sup> that a relaxation time much longer than 12 sec would be expected. The impurity mechanism is therefore reasonably excluded for all the measurements reported here, in view of the fact that the Na<sup>23</sup> relaxation time is the longest relaxation time measured in our experiments.

3. The temperature dependence of  $T_1$  for Na<sup>23</sup> in NaCl, Br<sup>79,81</sup> in KBr, and I<sup>127</sup> in KI shows that  $T_1$  is inversely proportional to the square of the absolute temperature. Quadrupole relaxation theories<sup>1,2</sup> predict a  $T^{-2}$  dependence above the Debye temperature because they utilize Raman processes to describe the nuclear quadrupole lattice-phonon interactions.

The nature of quadrupole line broadening is evident in our experiments. The chlorine, bromine, and iodine resonance lines appear at least to be broadened completely to first order.<sup>12</sup> Moreover in the case of RbBr, some second-order broadening<sup>12</sup> was evident in the Br resonance line because of the poor signal-to-noise ratio encountered. This led to a large error in the experimental value of  $T_1$ . A pulse,  $t_w$  seconds wide, is able to excite a frequency spectrum of breadth  $1/t_w$ , which evidently was exceeded by the overall line width. Furthermore, even if the wings of the spectrum are partially excited, the decay from the wings dies out very quickly, mostly within the dead time of the receiver following a pulse.

### III. TRANSITION PROBABILITY EQUATIONS

The experimental relaxation times will be interpreted in terms of the ionic and covalent models in Sec. IV. It is first necessary to derive the relaxation equations that describe the detailed balance between spins involved in a given pair of levels and also spins of other pairs of levels which have slightly different spacing because of a small quadrupole splitting. A coupling among spins, via the dipole-dipole interaction, is assumed necessary to establish a common spin temperature.<sup>13</sup> For a quadrupole system, both  $\Delta m = \pm 1$  and  $\Delta m = \pm 2$  transitions are allowed and correspond, respectively, to relaxation rates  $W_1$  and  $W_2$ , as shown in Fig. 1. Quadrupole-lattice relaxation between the  $m = \pm 1/2$  levels is forbidden to first order. A spin-spin

relaxation rate  $W_0$  is introduced<sup>14</sup> to account for dipole-dipole coupling, allowing approach to a common spin temperature. We assume that spin-spin transitions which conserve both energy and angular momentum occur via this coupling at the characteristic rate  $W_0$ .

Consider the case for  $I=3/2$ . The number of spins in each of the four levels is given by  $a$ ,  $b$ ,  $c$ , and  $d$ . We define, for convenience, the population differences,

$$A = a - d, \quad \text{and} \quad B = b - c,$$

with  $A_0$  and  $B_0$  given as these differences at thermal equilibrium. Also, it is necessary to define a spin-spin transition rate per spin as

$$P = W_0/N,$$

where  $N$  is the total number of nuclei. Since  $\mu H_0/kT \ll 1$ , where  $\mu$  is the nuclear magnetic moment, we let  $a = b = c = d = N/4$  wherever these terms do not occur as differences among themselves, and write  $PN/4 = z$ . Then the rate equations are:

$$\dot{A} = A(-W_1 - W_2 - z) + B(W_1 - W_2 + 3z) + 2B_0(W_1 + W_2), \quad (1)$$

$$\dot{B} = A(W_1 - W_2 + 3z) + B(-W_1 - W_2 - 9z) + 2B_0(2W_2 - W_1).$$

Solutions of the form  $\exp(-mt)$  give

$$m = (W_1 + W_2 + \frac{5}{4}W_0) \pm [(W_1 - W_2 + \frac{3}{4}W_0)^2 + W_0^2]^{\frac{1}{2}}, \quad (2)$$

which exists for any linear combination of population differences observed. If the  $W_0$  process is neglected, the transient relaxation is described by<sup>15</sup>

$$C + D \exp(-2W_1 t) + E \exp(-2W_2 t), \quad (3)$$

where  $C$ ,  $D$ , and  $E$  are constants determined by initial conditions. It is necessary, however, in our experiments to include  $W_0$ , and under the assumption that  $W_0 \gg W_1, W_2$ , the transient relaxation is described by

$$C + D \exp[-\frac{2}{5}(W_1 + 4W_2)t] + E \exp(-\frac{5}{2}W_0 t). \quad (4)$$

All values of  $T_2$  in our experiments are of the order of 1

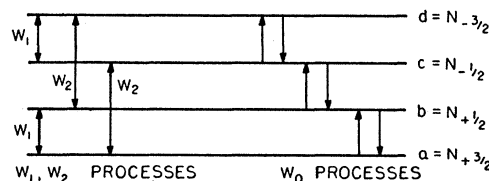


FIG. 1. Nuclear relaxation schemes for spin  $I = \frac{3}{2}$ , indicating spin-lattice quadrupole relaxation rates  $W_1$ ,  $W_2$ , and the spin-spin relaxation rate  $W_0$ .

<sup>9</sup> N. Bloembergen, *Physica* **15**, 386 (1949).

<sup>10</sup> N. Bloembergen and P. Sorokin, *Phys. Rev.* **110**, 685 (1958).

<sup>11</sup> W. E. Blumberg, Ph.D. thesis, University of California, 1959 (unpublished).

<sup>12</sup> N. Bloembergen and T. J. Rowland, *Acta Met.* **1**, 731 (1953).

<sup>13</sup> A. Abragam and W. Proctor, *Phys. Rev.* **109**, 1441 (1958).

<sup>14</sup> E. F. Taylor and N. Bloembergen, *Phys. Rev.* **113**, 431 (1959). This paper labels  $W_0$  as  $P$ . The authors would like to thank Dr. Taylor for sending his results before publication.

<sup>15</sup> L. Cohen and F. Reif, *Solid-State Physics*, edited by F. Seitz and D. Turnbull (Academic Press, New York, 1958), Vol. 5.

millisecond and are considerably shorter than  $T_1$ . An order-of-magnitude estimate of  $W_0$  is given by  $1/T_2$ . Consequently, the resolution of our experimental apparatus was insufficient for the detection of the fast ( $5W_0/2$ ) component of relaxation. We therefore define  $T_1$  as  $\frac{2}{3}(W_1+4W_2)^{-1}$  for those nuclei with  $I=3/2$  [see reference 14, Eq. (15)]. This equation applies for either the pulse or c.w. measurement case. When the  $W_0$  process is not included, however, the pulse analysis yields Eq. (3) and the c.w. analysis yields  $T_1=(1/W_1)+(1/W_2)$ . It has been shown<sup>16</sup> that when a spin temperature assumption is introduced, the relaxation is characterized by a single rate which has the form,  $\text{const}(W_1+4W_2)$ . This form of the relaxation is obtained upon the assumption of a common spin temperature. The coupling parameter  $W_0$  provides the means by which the nuclear spins can approach a common temperature.

For the case of  $I=5/2$ , the relaxation analysis is similar but more complicated by the existence of 6 Zeeman levels. The form of the relaxation time equation will remain the same,<sup>16</sup> i.e.,  $T_1=\text{const}(W_1+4W_2)^{-1}$ , because of the spin temperature approximation. However, the  $I^{27}$  nucleus does not lend itself to any obvious interpretation based upon the ionic or covalent models, and its analysis will be excluded. It does appear, however, that the dominant relaxation mechanism of iodine is covalent in nature.

#### IV. QUADRUPOLE RELAXATION MECHANISMS

The many-electron wave function in a crystal, such as NaCl, may be written in the form  $(\lambda|A|+|B|)$ , where the determinant  $|A|$  of the wave function corresponds to a configuration of Na and Cl atoms, and the determinant  $|B|$  corresponds to a configuration of  $\text{Na}^+$  and  $\text{Cl}^-$  ions. The coefficient  $\lambda$  is a small number which is a measure of the amount of covalent bonding that exists between Na and Cl ions. As a first approximation,  $B$  can be called the ionic model wave function and  $A$  can be called the covalent model wave function. The latter function includes effects due to covalency arising both from charge transfer, where unoccupied excited states become occupied, as treated by Yosida and Moriya, and from overlap of electron wave functions describing states which are already occupied, as treated by Kanda and Yamashita.<sup>17</sup> In the ionic model the field gradient at a nucleus is produced by an external charge and the electron wave functions only serve to enhance the interaction between the nuclear quadrupole moment and this charge. This enhancement is usually referred to as the Sternheimer factor or anti-shielding effect.<sup>3,18</sup> The problem becomes quite com-

<sup>16</sup> L. C. Hebel and C. P. Slichter, Phys. Rev. **113**, 1504 (1959). The authors would like to thank Professor Slichter and Dr. Micher for bringing these points to their attention.

<sup>17</sup> J. Kanda and J. Yamashita, J. Phys. Chem. Solids **10**, 245 (1959). The authors would like to thank Dr. Kanda for sending these results before publication.

<sup>18</sup> R. M. Sternheimer, Phys. Rev. **95**, 736 (1954).

TABLE II. Calculated relaxation times based on an ionic model.

Nucleus	Crystal	$T_1$ (expt.) (sec)	$T_1$ (ionic) (sec)	$T_1$ (ionic+induced dipole mechanism) <sup>a</sup> (sec)
$\text{Na}^{23}$	NaCl	12	420	30
$\text{Na}^{23}$	NaBr	6	340	10.8
$\text{Na}^{23}$	NaI	5	350	2.8
$\text{Cl}^{35}$	NaCl	5.2	6.4	5.8
$\text{Cl}^{35}$	KCl	8.5	12.5	7.0
$\text{K}^{39}$	KCl	6.2 <sup>b</sup>	202	28
$\text{Br}^{79}$	NaBr	0.052	0.095	0.082
$\text{Br}^{79}$	KBr	0.072	0.244	0.133
$\text{Br}^{79}$	RbBr	0.065±0.040	0.252	0.098
$\text{Br}^{79}$	CsBr	0.084	0.545	0.183
$\text{Rb}^{87}$	RbCl	0.250	4.51	0.845
$\text{Rb}^{87}$	RbBr	0.165	4.8	0.510
$\text{I}^{127}$	NaI	0.012	0.039 <sup>c</sup>	0.028
$\text{I}^{127}$	KI	0.019	0.091 <sup>c</sup>	0.043
$\text{I}^{127}$	CsI	0.010	0.172 <sup>c</sup>	0.060

<sup>a</sup> See Sec. IV, subsection B.

<sup>b</sup> Relaxation time estimated from Kanda's measured ratio for  $T_1(\text{K}^{39})/T_1(\text{Cl}^{35})$  in KCl of 0.73 (reference 17).

<sup>c</sup> Assumed  $T_1=\frac{5}{2}(W_1+4W_2)^{-1}$  and equal quadrupole moment matrix elements.

plicated if the relaxation theory is treated in a rigorous fashion by including cross-term effects between  $\lambda|A|$  and  $|B|$ . These cross terms arise since the total wave function occurs squared in the transition probability expression.

#### A. The Ionic Model

The nearest-neighbor ions in alkali halides are considered by Van Kranendonk<sup>1</sup> to be effective in causing relaxation. The acoustic modes of the Debye spectrum are assumed to describe the phonon distribution in which the "second-order" Raman processes are the most important. The expression for the transition probability from state  $m$  to  $m+u$  is given<sup>1</sup> by

$$W(m, m+u) = \gamma^2 |Q_{um}|^2 C T^{*2} E_u(T^*), \quad (8)$$

where  $C=27e^2/32\pi d^2 v^3 a^{13}$ ,  $d$  is the crystal density,  $v$  is the velocity of sound,  $a$  is the nearest-neighbor distance,  $T^* \equiv T/\Theta$  is the reduced temperature,  $\Theta$  is the Debye temperature,  $Q_{um} = \langle m+u | Q_u | m \rangle$  is the nuclear quadrupole moment matrix element, and  $E_u(T^*)$  is given by

$$E_{\pm 1}(T^*) = 1330(1 - 0.0056/T^{*2}), \quad (9)$$

$$E_{\pm 2}(T^*) = 476(1 - 0.0056/T^{*2}),$$

for  $T^* > 0.5$ . The  $\gamma$  is introduced by assuming that the actual ionic charge is  $q = \gamma e$ , where  $e$  is the electronic charge, and the parameter  $\gamma$  is a measure of the nuclear quadrupole-lattice coupling. Following Wikner and Das,<sup>3</sup> we shall write  $\gamma = 1 - \gamma_\infty$ , where  $\gamma_\infty$  is defined as the enhancement factor for the interaction of the nuclear quadrupole moment with the external charge. The enhancement is caused by the distortion of the electron cloud about the nucleus. Using Eq. (8) and  $T_1 = \frac{5}{2}(W_1+4W_2)^{-1}$ , the results are tabulated in Table II. The constants used in these expressions are given in Table III. With the above expression for  $T_1$ , Van

Kranendonk's theory predicts no  $T_1$  anisotropy,<sup>19</sup> i.e.,  $T_1$  does not depend on which direction the  $H_0$  field is applied to the crystal. This fact is verified by our experiments. It must be kept in mind, however, that any theory that uses the charge symmetry assumed in the ionic model will predict the same result.

For the Na<sup>23</sup> and K<sup>39</sup> nuclei there is a marked disagreement between the theory based upon the acoustic ionic model of Van Kranendonk and the experimental values. On the other hand, the acoustic ionic model provides reasonable agreement with the relaxation times measured for chlorine and bromine. Consideration of the induced dipole moment associated with the optical modes in addition to the acoustical modes in the ionic model serves to correct the serious discrepancies for Na and K relaxation data. Calculations which follow are carried out for the Cl and Br salts of Na, K, and Rb. There is overall agreement between the following theory and experiment within a factor of two.

### B. The Induced Dipole Mechanism

Optical vibrations produce large internal electric fields inside a crystal, which in turn induce electric dipole moments in the electronic shells of the ions.<sup>20</sup> These electric dipole moments produce strong electric field gradients at the sites of neighboring ions. A theory will be developed for the interaction of the nuclear quadrupole moment with the electric dipole moment induced by optical vibrations. This interaction will be incorporated into the calculation of Van Kranendonk, and the result will be applied to some crystals in which covalent effects can be neglected.

The polarization per unit volume produced by an optical vibration may be written as the sum of three parts, viz.,

$$\mathbf{P} = \mathbf{P}_+ + \mathbf{P}_- + Ze(\mathbf{u}_+ - \mathbf{u}_-)a^{-3}. \quad (10)$$

The displacements of all the positive and negative ions in a given region of the NaCl type crystal have been written as  $\mathbf{u}_\pm$ , assuming a long wavelength disturbance, and the induced polarization in the positive and negative ions is written as  $\mathbf{P}_\pm$ .  $Z$  is the valence of a positive ion. Figure 2 will serve to illustrate these three parts of the polarization. The scale of the drawing is appropriate to the KCl lattice, and the small circles represent the positive ions. The mid-section shows schematically a short wavelength acoustical wave. Note that each ion is shown with the nucleus in the center of the electronic shell, and that no dipole moments are induced by this type of vibration. On the right is shown a long wavelength optical wave. The last term in (10) is illustrated by a gross movement of charge. The

<sup>19</sup> The authors would like to thank Dr. Mieher and Professor Slichter for bringing this to our attention. Mieher and Slichter will soon publish a paper which will discuss this problem to a greater extent.

<sup>20</sup> M. Born and K. Huang, *Dynamical Theory of Crystal Lattices* (Clarendon Press, Oxford, 1954).

TABLE III. Crystal and nuclear constants used in relaxation time calculations.

	Lattice spacing <sup>a</sup> $a$ (Å)	Velocity of sound <sup>b</sup> $v$ (m/sec)	Density $d$ (g/cm <sup>3</sup> )	Debye temp. <sup>c</sup> $\Theta$ (°K)
NaCl	2.815	4738	2.165	281
NaBr	2.98	3330	3.203	200
NaI	3.23	(2600) <sup>d</sup>	3.667	151
KCl	3.14	4490	1.984	227
KBr	3.29	3570	2.75	177
KI	3.52	2940	3.13	130
RbCl	3.27	(3600) <sup>d</sup>	2.76	179
RbBr	3.43	(3100) <sup>d</sup>	3.35	140
CsBr	3.71	(2600) <sup>d</sup>	4.44	(125) <sup>d</sup>
CaI	3.95	(2100) <sup>d</sup>	4.51	95

	Antishielding factor <sup>e</sup> $\gamma_\infty$	$\langle 1/r^3 \rangle$ values <sup>f</sup> $\langle 1/r^3 \rangle \times 10^{24}$	Atomic polarizabilities <sup>g</sup> $\alpha_\pm$
Na	— 4.5	1.66	0.28
K	— 12.84	2.98	1.13
Rb	— 49.3	5.74	1.79
Cl	— 49.4	48.64	2.92
Br	— 99	92.05	4.12
I	— 179	122.3	6.41
Cs			2.85

<sup>a</sup> R. W. G. Wyckoff, *Crystal Structures* (Interscience Publishers, Inc., New York, 1951), Vol. 1. Here " $a$ " is the nearest-neighbor distance, not the lattice constant  $a_0$ .

<sup>b</sup> Calculated from elastic constant data, viz.,  $v = (C_{11}/d)^{1/2}$ , where  $C_{11}$  is the longitudinal elastic constant, and  $d$  is the density.

<sup>c</sup> K. Lonsdale, *Acta Cryst.* 1, 144 (1948).

<sup>d</sup> See reference 3.

<sup>e</sup> R. G. Barnes and W. V. Smith, *Phys. Rev.* 93, 95 (1954).

<sup>f</sup> See M. Born and K. Huang, *Dynamical Theory of Crystal Lattices* (Clarendon Press, Oxford, 1954).

<sup>g</sup> Estimated values.

positive ions are shown displaced downward, and the negative ions are displaced upward. This produces an effective field in the upward direction, with the result that the negatively charged electronic shells of both kinds of ions are displaced downward with respect to the nucleus. This has caused a dipole moment to be introduced in each ion.

Assume the ionic polarization can be written as

$$\mathbf{P}_\pm = \alpha_\pm \mathbf{E}_{\text{eff}} a^{-3}, \quad (11)$$

where  $\mathbf{E}_{\text{eff}}$  is an effective local electric field acting on the positive and negative ions alike, and  $\alpha_\pm$  is the electric polarizability of the positive or negative ions in the crystal.<sup>21</sup> Then the induced dipole moment of an ion may be expressed as

$$e\mathbf{u}_\pm = \mathbf{P}_\pm a^3 = \frac{\alpha_\pm [\mathbf{P} a^3 - Ze(\mathbf{u}_+ - \mathbf{u}_-)]}{\alpha_+ + \alpha_-}. \quad (12)$$

It is now necessary to calculate  $\mathbf{P}$  as a function of the relative displacement  $\mathbf{u}_+ - \mathbf{u}_-$ . In the absence of an externally applied electric field, the effective Lorentz field at any point in the crystal is given by

$$\mathbf{E}_{\text{eff}} = (4\pi/3)\mathbf{P}. \quad (13)$$

The effective field can be eliminated from (11), (12),

<sup>21</sup> W. Shockley, *Phys. Rev.* 70, 105 (1946).

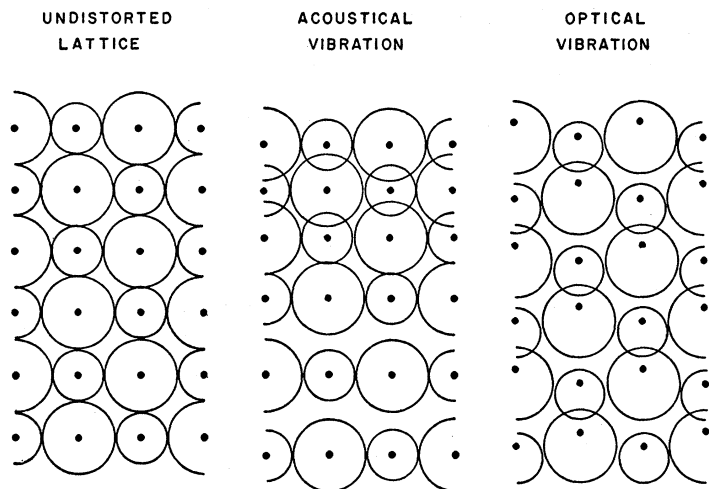


FIG. 2. Schematic representation of an acoustic and an optical vibration emphasizing the distortion of the ions which occurs during an optical vibration. The scale is appropriate to KCl, the positive ions being represented by the smaller circles.

and (13), to obtain

$$\mathbf{P} = \frac{Ze(\mathbf{u}_+ - \mathbf{u}_-)}{a^3 - (4\pi/3)(\alpha_+ + \alpha_-)} \quad (14)$$

The magnitude of the displacement is now written as  $\epsilon$ . Then the magnitude of the induced dipole moment is

$$e\mu_{\pm} = Ze\epsilon \left[ \frac{1}{1 - (4\pi/3)(\alpha_+ + \alpha_-)a^{-3}} \right] \frac{\alpha_{\pm}}{\alpha_+ + \alpha_-} \quad (15)$$

Because of the assumed isotropy of the crystal, the direction of the dipole moment is parallel to the relative displacement of the positive and negative ions.

Any effects of the electric field gradient at the nucleus of an ion caused by the electric dipole deformation of that ion are considered to be negligible. This is presumed to be generally true, based upon a calculation by Sternheimer<sup>18</sup> for the  $\text{Cl}^-$  ion, in which the field gradient at the chlorine nucleus, caused by an electric field acting to polarize the ion shell, occurs only as a second-order perturbation. The interaction with the nuclear quadrupole moment depends upon the square of the electric field and, therefore, upon the square of the displacement. For the small displacements caused by thermal vibrations, this interaction may be neglected in comparison with the field gradient caused by a dipole deformation of a neighboring ion, which depends linearly upon displacement.

The treatment and notation of Van Kranendonk are followed in the evaluation matrices for the strength of the interaction of the nuclear quadrupole moment with the surrounding ions. However, some different assumptions concerning the nature of the crystal must be made. Since the main interest lies in the relaxation due to the optical modes of vibration, it cannot be assumed that the nuclei are all equivalent. A perfect NaCl-type lattice of alternating positive and negative ions is assumed, which has dipole polarizabilities  $\alpha_+$  and  $\alpha_-$ , respectively. The frequency distribution of

phonons is taken to be the Debye spectrum. This is probably not the most realistic spectrum to assume, but it is chosen for convenience in comparing the results with those for the case of relaxation due to acoustical vibrations using the Debye spectrum. The integrated spectrum of optical vibrations is comparable to that of acoustical vibration, so that this assumption is sufficient in view of errors inherent in other parameters chosen. The greatest portion of the optical phonons have  $1/k_0 \gg a$ , where  $k_0 = 2\pi/\lambda$  is the magnitude of the reciprocal wave vector, and those phonons for which  $1/k_0$  is comparable to the lattice constant play a negligible role in the relaxation process. However, just the opposite is true in the case of acoustical phonons, as treated by Van Kranendonk, where the acoustical phonons for which  $1/k_0 \approx a$  contributed most to the relaxation. Under these assumptions, we may write the matrix elements of the perturbing Hamiltonian as

$$|3C_2'| = \gamma^2 (2\hbar Q_{um}/M\omega) [n_{\omega}(n_{\omega}+1)N_u]^{\frac{1}{2}}, \quad (16)$$

where  $n_{\omega}$  is the number of quanta at frequency  $\omega$ ,  $M$  is the mass of the crystal, and the required values of  $N_u$  are computed to be

$$N_1 = 5292(d\mu/d\epsilon)^2 a^{-10}, \text{ and } N_2 = 8140(d\mu/d\epsilon)^2 a^{-10}, \quad (17)$$

for the case in which the magnetic field is along a [100] direction in the crystal. Then the expression for the transition probability becomes

$$W(m, m+u) = \frac{2\pi}{\hbar^2} \int_0^{\omega_m} \left( \frac{3\omega^2 \hbar^3 V}{4\theta^3 k_0^3 a^3} \right)^2 \left[ \frac{2\hbar \exp \hbar\omega/kT}{M\omega(\exp \hbar\omega/kT - 1)} \right]^2 \times N_u \gamma^2 |Q_{um}|^2 e^2 d\omega, \quad (18)$$

where  $V$  is volume of the crystal and  $\omega_m$  is the Debye cutoff frequency.

In order to facilitate a comparison with the theory of Van Kranendonk, it is desirable to write the expres-

sion for  $W$  in the form,

$$W(m, m+u) = \gamma^2 |Q_{um}|^2 C E_u T^{*2} E'(T^*) (d\mu/d\epsilon)^2, \quad (19)$$

where  $C$  is the same as in Eq. (8). The function  $E_u$  is the result of all the geometrical factors governing the coefficient of  $Q_{um}$  in the matrix elements of  $\mathcal{H}_2'$ . The function  $E'(T^*)$  here is not quite the same as defined by (9). It is here defined as

$$E'(T^*) = T^* \int_0^{1/T^*} \frac{e^{xz} dx}{(e^x - 1)^2}. \quad (20)$$

The relation

$$k_0 \theta a = (6\pi^2)^{1/2} \hbar v \quad (21)$$

may be used to introduce the velocity of acoustic waves into (18). The values of  $E_u$  for this case are  $E_1 = 4704$ ,  $E_2 = 7236$ .

Now the results of the induced dipole process may be combined with the results of the acoustic case for a nuclear spin of  $3/2$ . For this case, the values of  $W(m, m+u)$  are the same for all values of  $m \leq 3/2 - u$  [except  $W(-1/2, 1/2) = 0$ ] and may be written as  $W_u$ . The combined relaxation rate due to both modes of vibration is

$$1/T_1(\text{total}) = \gamma^2 Q^2 C T^* [1806 E^* + 11,940 (d\mu/d\epsilon)^2 E'], \quad (22)$$

where  $E^*$  and  $E'$  are given by Eqs. (9) and (20), respectively. Here it is assumed that the antishielding factor for each process is the same.<sup>22</sup> Since covalent effects are neglected, and since the electric field gradient acting on a given ion arises entirely from a charge configuration lying entirely outside that ion, it is assumed that the shielding theory of Sternheimer<sup>18</sup> holds. Relaxation times  $T_1(\text{total})$  are computed by first obtaining the value of  $d\mu/d\epsilon$  from (15) using the values of the crystal polarizabilities computed by Shockley.<sup>21</sup> At room temperature, the values of both  $E^*(T^*)$  and  $E'(T^*)$  are approximately unity and

$$\frac{1}{T_1} = [1 + 6.62 (d\mu/d\epsilon)^2] \frac{1}{T_1(\text{acoustic})}. \quad (23)$$

Because of the large number of simplifying assumptions made in the theory of relaxation caused by a Debye spectrum for both phonons and optical phonons, the factor  $6.62 (d\mu/d\epsilon)^2$  should not be taken too literally.

Some calculations based on (22) are presented in Table II. The lithium halides and alkali fluorides have been omitted from consideration, as relaxation does not proceed entirely via the nuclear quadrupole moment in these compounds at room temperature. The cesium halides and the alkali iodides have been omitted for two reasons. The nuclear spins of both Cs<sup>133</sup> and I<sup>127</sup> are greater than  $3/2$ , so the relation

<sup>22</sup> This is justified in a paper by G. Burns and E. G. Wikner (to be published).

employed in Eq. (4) does not apply. In addition, there is possibly some effect on the relaxation time caused by the partial covalency exhibited by these large ions, especially I<sup>127</sup>. Results for only one of the isotopes of Cl, Br, and Rb have been shown for each element. The calculated relaxation times for the other isotopes of Cl and Br may be obtained by multiplying the listed results by the appropriate inverse square of the ratio of quadrupole moments.

It can be seen from Table II that the values of the relaxation time for the halide negative ion nuclei are not greatly changed upon addition of the optical phonon process. The values for the alkali positive ion nuclei, however, show marked reduction in relaxation times because of the large polarizability of the neighboring negative ions. Thus the importance of the optical phonons in the nuclear magnetic relaxation process has been demonstrated approximately, whereby the nuclear Zeeman energy is taken up by the lattice vibrations through an interaction of the nuclear quadrupole moment with the time-varying electric field gradient arising from ionic and lattice distortion caused by optical phonons. The inclusion of this relaxation process places the calculated values for the relaxation times for each crystal studied in the range of experimentally determined values of relaxation times. We notice, however, that there is still some disagreement between theory and experiment in the case of the heavier nuclei. Some of the disagreement might be ascribable to the calculated antishielding factor. The cubic environment of the nuclei precludes any large effect on  $\gamma_\infty$  by the crystalline fields themselves. The crystalline environment, on the other hand, will modify the free ion wave function used in the  $\gamma_\infty$  calculations since the wave function will not now extend as far out. The result of this will be to lower the radial wave function expectation values leading to a decrease in  $\gamma_\infty$ . Burns<sup>22</sup> has computed this effect for Cl<sup>-</sup> and finds that  $\gamma_\infty$  decreases from 50 to 27. Also, ultrasonic measurements,<sup>14,28,24</sup> second-order broadening effects,<sup>25</sup> and field gradient calculations<sup>26</sup> all tend to show that  $\gamma_\infty(\text{calc})$  is fairly reliable for the positive ions, but is too large for the negative ions. Modified values of  $\gamma_\infty$  for the negative ion, assuming  $\gamma_\infty$  for positive ions unchanged, can be predicted from the measurement of relaxation time ratios of different ions in the same crystal. Assuming  $\gamma_\infty$  for Na to be 5, the modified ionic model for relaxation times predicts a  $\gamma_\infty$  of 20 for Cl, again a smaller value than computed.

The calculated values of  $\gamma_\infty$  for bromine and iodine are uncertain in the original calculation<sup>8</sup> because interpolated wave functions without exchange were used. It appears that  $\gamma_\infty$  calculated on this basis is

<sup>23</sup> D. A. Jennings, W. H. Tantilla, and O. Kraus, Phys. Rev. **109**, 1059 (1958).

<sup>24</sup> D. I. Bolef and M. Menes, Phys. Rev. **114**, 1441 (1959).

<sup>25</sup> E. Otsuka and J. Kawamura, J. Phys. Soc. (Japan) **12**, 1071 (1957).

<sup>26</sup> R. Bersohn, J. Chem. Phys. **29**, 362 (1958).

overestimated, since Burns has shown for chlorine that the ratio of  $\gamma_\infty$  (using Hartree wave functions) to  $\gamma_\infty$  (using Hartree-Fock wave functions) is 3.1, which demonstrates the importance of exchange in reducing the value of  $\gamma_\infty$ .

The  $T_1$  data for the bromine sequence in Table II shows a steadily increasing discrepancy between theory and experiment through the series NaBr, KBr, and CsBr. (RbBr is omitted here because of the large inaccuracy in its  $T_1$  measurement.) The ratio  $T_1$ (calculated) to  $T_1$ (experimental) for Br<sup>79</sup> is 1.13, 1.32, and 1.56, respectively for this series. If we also consider iodine, we find that in passing from KI to CsI, a decrease in  $T_1$  occurs for I<sup>127</sup> which is not predicted by the ionic model. This trend can be accounted for by introducing covalency effects for the heavier atoms.

### C. The Covalent Model

Thus far the perturbing influences of the electron charge transfer and overlap of electron wave functions have been neglected. For a given anion X, these perturbing influences will increase along the series NaX, KX, and CsX and thereby lead to a decrease in  $T_1$  along this series.

#### 1. Theory of Yosida and Moriya

This theory<sup>2</sup> is based upon a covalent crystal model and differs from the ionic picture only in the mechanism which produces the field gradient. The same assumptions concerning lattice vibrations (Debye model, etc.) and nearest-neighbor interactions are employed. For an ion with completed electronic shells, the charge distribution around the nucleus is spherically symmetric. But in a state of covalent bonding, there is a small charge transfer and the asymmetry caused by this transfer in the closed shell configuration generates an electric field gradient proportional to  $\langle r^{-3} \rangle_p$  at the position of the nucleus. The subscript  $p$  refers to the outermost  $p$  state of the ion in question. Based on this model, Yosida and Moriya obtain the following expression for the transition probability equations:

$$W(m, m+u) = A'^2 c_0 |Q_{um}|^2 T^{*2} \sum_{n=1}^4 N_{un} D_n(T^*), \quad (24)$$

where  $A' = \frac{2}{3} eA \langle r^{-3} \rangle_p$ ,  $A = eQ/I(2I-1)$ ,  $c_0^3 = (6\pi^2)$  for sc crystals, and  $c_0^3 = 9\sqrt{3}\pi^2/2$  for bcc crystals. The  $D_n(T^*)$  terms have the form  $(x+y)T^{*-2}$ , where  $x$  and  $y$  are constants. The  $N_{un}$  terms have the form

$$N_{un} = \lambda^2 [a + b(\lambda'/\lambda) + c(\lambda'/\lambda)^2 + d(\lambda''/\lambda)], \quad (25)$$

where  $a$ ,  $b$ ,  $c$ , and  $d$  are numerical constants,  $\lambda$  is the degree of covalency obtained from chemical shift data,<sup>2</sup> and  $\lambda'$  and  $\lambda''$  are, respectively, the first and second derivatives of  $\lambda$  with respect to the interionic distance. These derivatives arise since Raman processes, which are of second order, are used in describing the nuclear

quadrupole-lattice interactions. These are estimated by assuming  $\lambda \sim \exp(-r/0.345)$ , after Born and Mayer, where  $r$  is the interionic distance. The representation of the excited covalent-state wave functions by such a simple exponential term is, of course, only a first approximation. This approximation is crude since the value of  $N_{un}$  is essentially dominated by the magnitude of the  $\lambda''$  term. To improve this model, however, would require an accurate knowledge of the electron distribution near the peripheral regions of the ion, and hence a band structure calculation is necessary to obtain the electron wave functions. Another point to consider is the phenomenon of double repulsion among the cations. In the Li and Na halide crystals especially, the disparity in ionic sizes between the alkalis and halides allows the like-charged halides to overlap, thus enhancing the repulsive forces they experience. This will further increase the distortion of the electron charge density for these crystals, and therefore a nearest-neighbor model is insufficient. The inclusion of next nearest neighbors could be carried out by a difficult and involved band-structure calculation.

The formula relating the chemical shift to the degree of covalency is based on the same model used in the covalent relaxation theory. However, for crystals composed of large ions, such as the cesium halides, the chemical shift formula should be modified to include bonding  $d$  orbitals. This would be especially true for nuclei which exhibit a comparatively large chemical shift, such as Br in CsBr and I in CsI (see Table IV). Undoubtedly this is the cause of some of the discrepancies that arise in the calculations to follow.

In Table IV are listed the measured chemical shifts  $\sigma$ ; the degree of covalency  $\lambda$ ; the energy of excitation  $\Delta E$  between ground and excited states, as deduced by Yosida and Moriya,<sup>2</sup> and Kanda and Yamashita<sup>17</sup>; the relaxation times as calculated from Eq. (24); and the experimental relaxation times. The degrees of covalency listed in parentheses are estimates, because the formula relating the chemical shift to the degree of covalency assumes a negative shift while these ions exhibited a positive shift. A positive shift most likely means the reference point is somewhat uncertain and the assumption that the reference aqueous salt solution is completely ionized is not entirely correct. The theoretical ratio  $T_1(\text{Na})/T_1(\text{Cl}) = R$  in NaCl, obtained from Table IV, is about 500 as compared to the measured  $R$  of about two. The great difference in these ratios is accounted for by the respective  $\langle r^{-3} \rangle$  values (see Table III) of Na and Cl obtained from hyperfine-structure data, where corrections due to the Sternheimer polarization effects on the atomic core are neglected. These are usually important and would be expected to modify the tabulated  $\langle r^{-3} \rangle$  values. However, to obtain a "correct" theoretical  $R$  in NaCl, the  $\langle r^{-3} \rangle$  value for Na would have to be increased by a factor of 10 which is rather unreasonable for this tightly bound ion. It would also be unreasonable to choose a higher covalent bond



TABLE IV. Calculated  $T_1$  values.<sup>a</sup>

(a) Calculated $T_1$ values based on the covalent model						
Nucleus	Crystal	Chemical shift $\sigma$ $\times (10^4)$	$\Delta E$ (ev)	$\lambda$	$T_1$ (calc) (sec)	$T_1$ (exp.) (sec)
Na <sup>23</sup>	NaCl	none	...	(0.01) <sup>b</sup>	$2.3 \times 10^3$	12
Na <sup>23</sup>	NaBr	observed none	...	(0.01) <sup>b</sup>	$2 \times 10^3$	6
Cl <sup>35</sup>	NaCl	+0.3	...	(0.01) <sup>b</sup>	4.4	5.2
Br <sup>79</sup>	NaBr	+0.58	...	(0.002) <sup>b</sup>	2	0.050
Br <sup>79</sup>	KBr	-0.22	10.1	0.004	0.190	0.072
Br <sup>79</sup>	CsBr	-2.5	9.4	0.02	0.002	0.080
Rb <sup>87</sup>	RbCl	-0.9	20	0.007	0.012	0.250
Rb <sup>87</sup>	RbBr	-1.29	20	0.0083	0.003	0.165
I <sup>127</sup>	NaI	-1.2	9.0	0.0091	See part (b) below	
I <sup>127</sup>	KI	-1.0	9.0	0.0076	See part (b) below	
I <sup>127</sup>	CsI	-5.0	8.4	0.0284	See part (b) below	

(b) Ratios of I <sup>127</sup> relaxation times $T_1$ in KI and CsI to that of I <sup>127</sup> in NaI				
	NaI	KI	CsI	
Expt.	1	1.6	0.83	
Covalent (calc)	1	1.57	0.04	
Ionic (calc)	1	1.5	3.6	

<sup>a</sup> The Br and I shifts are obtained from reference 10. The Rb data are obtained from reference 17.  $\Delta E$  is obtained from reference 2.

<sup>b</sup> Estimated values.

character for the Na ion, since, for Br in KBr, which exhibits a larger chemical shift, the covalent character is only 0.4% per bond. The essential arguments are the same for NaBr, and thus it is apparent that the charge transfer covalent model is inadequate in explaining the observed relaxation times in these crystals. For the Br sequence, it is evident that the spin-lattice relaxation of Br in NaBr is dominated by an ionic process, because the amount of covalent bond character (2.84%) needed to give agreement is much too high (the CsBr bond character is only 2%). The dominating relaxation process in KBr is difficult to determine, but certainly in CsBr it is covalent in nature. Also, as mentioned previously, the I<sup>127</sup> nuclear quadrupole relaxation process also appears to be dominantly covalent in nature.

### 2. Theory of Overlap Covalency

Recently, Kanda and Yamashita<sup>17</sup> have calculated the influence of the overlap covalency, arising from the

so-called "exchange effect" alone, on the nuclear quadrupole spin-lattice relaxation. The charge distribution around an ion is nonspherical because of the mutual overlap of the electron charge clouds of nearest-neighbor ions. This distribution provides a field gradient at the nucleus which is modulated by the lattice vibrations. It differs mainly from the Yosida and Moriya theory in the appearance of an overlap integral between the metal and halogen orbitals, instead of the covalency, and in the case of the metal ion, there appears the value of  $\langle r^{-3} \rangle$  for an occupied orbital instead of the excited outer orbital. The relaxation times for the alkali and halogen nuclei then become of the same order of magnitude. We learned of the results of Kanda and Yamashita near the end of our investigation and therefore did not include their mechanism in the prediction of relaxation due to covalency.

## V. CONCLUSIONS

It appears that the predominant contribution to the relaxation times is neither covalent nor ionic, but that both effects must be considered. When dealing with relaxation processes it is not valid to consider the crystals studied here as being purely ionic in character. However, the theory for the ionic model, based on the original calculation of Van Kranendonk, and later modified to include the antishielding factor and the induced dipole polarization, is better established than the covalent model. The latter has been only incompletely studied at this point by virtue of the neglect of the overlap covalency and the treatment of the charge transfer calculation of Yosida and Moriya. Although the two conditions, ionic and covalent, may be in some cases of equal importance in contributing to the relaxation mechanism, considerable improvement is necessary in the covalent theory.

## ACKNOWLEDGMENTS

The authors wish to thank Dr. T. P. Das for many helpful discussions and suggestions. We are indebted to Dr. J. Phillips for the suggestion that the optical modes of vibration might be important in the treatment of quadrupole relaxation.